Scientia Horticulturae 165 (2014) 148–155

Contents lists available at ScienceDirect

Scientia Horticulturae

journal homepage: www.elsevier.com/locate/scihorti

Chlorophyll fluorescence imaging as a tool to understand the impact of iron deficiency and resupply on photosynthetic performance of strawberry plants

Júlio Osório[a,*], Maria Leonor Osório[b], Pedro José Correia[a], Amarilis de Varennes[c], Maribela Pestana[a]

[a] Institute of Mediterranean Agricultural and Environmental Sciences – (ICAAM), Faculty of Sciences and Technology, University of Algarve, Ed. 8, Campus de Gambelas, 8005-139 Faro, Portugal
[b] Institute for Biotechnology and Bioengineering, Centre of Genomics and Biotechnology (IBB-CGB), Faculty of Sciences and Technology, University of Algarve, Ed. 8, Campus de Gambelas, 8005-139 Faro, Portugal
[c] Biosystems Engineering Center, Instituto Superior de Agronomia, University of Lisbon, Tapada da Ajuda, 1349-017 Lisbon, Portugal

ARTICLE INFO

Article history:
Received 8 February 2013
Received in revised form 31 July 2013
Accepted 29 October 2013

Keywords:
Chlorophyll fluorescence imaging
Energy partitioning
Fragaria × ananassa
Iron deficiency
Photosynthetic efficiency

ABSTRACT

Bare-root transplants of strawberry (Fragaria × ananassa Duch. cv 'Diamond') were grown in a Hoagland's nutrient solution with or without Fe. Forty two days after Fe deprivation, recovery was induced by addition of 10 μM of Fe (Fe-EDDHA) to the Fe(−) nutrient solution. Total leaf chlorophyll concentration in young leaves decreased progressively with time in Fe-deprived plants, and before Fe resupply it was only 6% of that of Fe(+) control plants. Spatio-temporal changes on photosynthetic efficiency were monitored by imaging chlorophyll a fluorescence in four areas of interest (AOIs) located on the midrib and on interveinal mesophyll areas of leaf blades. Chlorophyll fluorescence images (F_v/F_m, ϕ_{II}, NPQ, q_p) showed a large spatial variation, particularly at day 42, with greater values in midrib areas. Temporal changes were also observed in all measured parameters along the experimental period, but the onset and intensity of impact was clearly different between parameters. Maximal efficiency of PSII (F_v/F_m) was the last parameter to be affected, being the effects visible only in plants that had lost over 90% of their chlorophyll (day 42). In contrast, actual efficiency of PSII (ϕ_{II}) and photochemical quenching (q_p) were affected earlier on, showing noticeable changes by day 20, when chlorophyll concentration had declined by 38%. Decreases in ϕ_{II} were balanced by increases in quantum yield of non-regulated energy dissipation (ϕ_{NO}). Fluorescence parameters, with the exception of ϕ_{II} and Fe content, recovered within eight days following Fe resupply to values found in Fe(+) plants. The results of this study indicate that: (i) Chl fluorescence imaging is a useful technique to evaluate Fe deficiency (ii) Fe stress generates spatio-temporal heterogeneity in fluorescence response (iii) ϕ_{II} measured in interveinal mesophyll areas could be used as an early and fast indicator of Fe deficiency and could be applied for fertilization management.

1. Introduction

Iron (Fe) deficiency is a well-documented problem affecting crop production worldwide, in particular in calcareous soils of Mediterranean basin countries, including Portugal (Pestana et al., 2004). Fe-deficient plants are characterized by the development of a pronounced chlorosis occurring first on the youngest leaves and causing various morphological and physiological changes in plants. Among other effects, Fe deficiency affects the structure, development and function of the entire photosynthetic apparatus (Terry and Abadía, 1986; Abadía et al., 1999). It has been shown that Fe deficiency leads to decreases in light-harvesting pigments, particularly chlorophylls (Morales et al., 2000), and promotes antenna disconnection in PSII (Morales et al., 2001, Moseley et al., 2002). Furthermore, Fe-deficient leaves show lower actual PSII efficiency (ϕ_{II}) and a decrease in the proportion of open PSII reaction centers (q_p) (Larbi et al., 2006). However, many abiotic stresses, including Fe deficiency, do not result in uniform symptoms, but rather on patches of visible injuries on leaf surfaces, more drastic in mesophyll leaf areas than in midrib and veins in the case of this deficiency. It was also shown that Fe-deficient leaves accumulated more Fe in the midrib and veins, with lower Fe concentration in mesophyll leaf areas (Jiménez et al., 2009; Tomasi et al., 2009). Thus, this heterogeneous distribution of photosynthetic pigments and Fe in leaves could equally affect the photosynthetic efficiency.

* Corresponding author. Tel.: +351 289 800900; fax: +351 289 818419.
E-mail address: josorio@ualg.pt (J. Osório).

0304-4238/$ – see front matter © 2013 Elsevier B.V. All rights reserved.
http://dx.doi.org/10.1016/j.scienta.2013.10.042

In recent years, chlorophyll (Chl) fluorescence analysis has been applied as a rapid non-destructive tool to obtain information about the state of photosynthetic apparatus and especially of photosystemII (PSII). One of the major disadvantages of conventional Chl fluorescence measurements is that it provides information only on a single leaf spot, which is not representative of the physiological status of the whole leaf (Lichthentaler and Miehé, 1997). The development of instruments capable of imaging Chl fluorescence provided a powerful tool to identify spatial heterogeneity of leaf photosynthetic performance, and offered new possibilities to understand the operation and regulation of photosynthesis (Baker, 2008; Gorbe and Calatayud, 2012). This rapid non-destructive method has been used to assess the effects of other abiotic stresses on photosynthetic efficiency (Calatayud et al., 2006; Osório et al., 2011, 2012, 2013; Martins et al., 2013). The use of Chl fluorescence imaging to quantify the degree of photosynthetic leaf heterogeneity related with Fe nutrition seems obvious, but to our knowledge this is the first report of such a study. As stressors can modify the partitioning of absorbed light energy in leaves, analysis of the contribution of different routes for excitation energy utilisation/dissipation in PSII complexes is of huge importance to study the regulatory mechanisms involved in responses of the photosynthetic apparatus (Kornyeyev and Hendrickson, 2007). Furthermore, this approach also allows a deeper insight into the plant's capacity to cope with excess excitation energy (Klughammer and Schreiber, 2008).

Various authors reported that Fe resupply to deficient plants restores many plant functions. For instance, it leads within a few days to increases in chlorophyll concentration and photosynthetic activity in several annual species, including sugar beet (Nishio et al., 1985; Larbi et al., 2004), soybean (Hecht-Buchholz and Ortmann, 1986) and tobacco (Pushnik and Miller, 1989). It was also recorded that tolerance to Fe deficiency may vary between different varieties of the same species, and the capacity to recover from this stress was related with sensitivity to the deficiency (Mahmoudi et al., 2007). However, knowledge on the responses of chlorotic plants to Fe resupply is still scarce, although it may provide crucial information to optimize Fe-fertilization strategies (Abadía et al., 2011; Pestana et al., 2012).

Strawberries are a major crop in southern Portugal where calcareous soils with high levels of bicarbonate ions tend to decrease Fe availability, representing a major constraint to their production. A deeper understanding of the development of Fe stress and plant recovery after resupply is essential to develop suitable and sustainable Fe-fertilization programs for crop production on calcareous soils.

In the present study, we evaluated the potential of Chl fluorescence imaging to investigate the effects of Fe deficiency and Fe resupply on spatial and temporal efficiency of PSII in *Fragaria × ananassa* Duch. cv 'Diamond' grown in hydroponics. The specific aims of this work were: (i) to map leaf chlorosis across leaf blades of recently-expanded leaves; (ii) to assess the effects of Fe deficiency and Fe resupply on Chl and Fe concentrations throughout time; (iii) to check whether high Chl and Fe concentrations in vascular tissues of Fe-deficient leaves would also result in high photosynthetic efficiency; (iv) to identify an early and fast chlorophyll fluorescence indicator for Fe deficiency and Fe recovery.

2. Material and methods

2.1. Plant material and experimental conditions

Experiments were carried out with a strawberry cultivar (*Fragaria × ananassa* Duch. cv 'Diamond') commonly cultivated in the Algarve, southern Portugal. Forty eight plants were cultivated in six

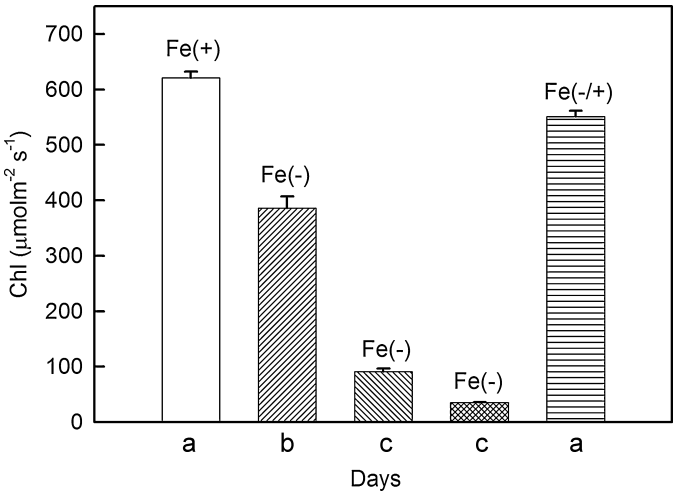

Fig. 1. Chlorophyll concentrations (Chl) as estimated by SPAD-502 meter during Fe treatments: moderately Fe-deficient (Fe(−)/Day 20), severely Fe-deficient (Fe(−)/Day 27), extremely Fe-deficient (Fe(−)/Day 42 and Fe-recovered plants (Fe(−/+)/Day 50). Fe(+) and Fe(−) indicate solutions with 10 μM of Fe (Fe-EDDHA) or 0 μM of Fe, respectively. Values shown are means ± SE of six measurements taken in five leaves per treatment. Different letters indicate significant differences between treatments ($P < 0.05$) according SNK test.

20-L poly-ethylene vessels filled with Hoagland's nutrient solution, which contained: 5 mM $Ca(NO_3)_2$, 5 mM KNO_3, 1.0 mM KH_2PO_4, 2.0 mM $MgSO_4$, 46.0 μM H_3BO_3, 0.8 μM $ZnSO_4$, 0.4 μM $CuSO_4$, 9.0 μM $MnCl_2$, and 0.02 μM MoO_3. Half of the plants were grown in the presence of 10 μM Fe added as Fe(III)-EDDHA, Fe(+), and half in the absence of Fe, Fe(−). The initial pH of the nutrient solution was 6.0 ± 0.2 and the electrical conductivity (EC) was 2.2 ± 0.1 dS m^{-1}. The aerated nutrient solution was replaced when the EC dropped to 1.7 dS m^{-1}. The experiments were performed in a glasshouse under natural photoperiod conditions: a photosynthetic photon flux density (PPFD) of 150 − 450 μmol m^{-2} s^{-1} at the top of the plants and a temperature ≤25 °C. After 42 days, Fe(+) plants remained green but Fe(−) plants were severely chlorotic (Fig. 1). At this point, in order to study recovery from Fe deficiency, half of the chlorotic plants were transferred to nutrient solution that contained Fe, and further grown for eight days. The treatments are described as follows: Fe-sufficient = Fe(+)/Day 0, moderately Fe-deficient = Fe(−)/Day 20, severely Fe-deficient = Fe(−)/Day 27, extremely Fe-deficient = Fe(−)/Day 42 and Fe-recovered plants = Fe(−/+)/Day 50. Measurements were taken on the youngest fully expanded leaves of five plants of each treatment. At the end of the experiment (a total of 50 days), the number of leaves and their fresh weights were registered.

2.2. SPAD readings, chlorophyll concentrations and Fe contents

The first new leaves appeared approximately 15 days after the beginning of the experiment and from then on the degree of chlorosis was estimated non-destructively in the youngest fully expanded apical leaves from five plants of each treatment using a portable SPAD-502 meter (Minolta, Osaka, Japan). Six SPAD readings were recorded for each leaf, homogeneously distributed from the apex to the base of the leaf, to obtain a representative degree of leaf chlorosis. SPAD readings were converted to total Chl using the calibration curve:

$$y = 0.45x^2 - 1.11x + 32.56 (R^2 = 0.98; n = 31; P < 0.001)$$

where y is the Chl concentration (μmol m^{-2}) measured spectrophotometrically and x is the SPAD readings measured in strawberry leaves (Pestana et al., 2011a).

At the end of the experiment, youngest leaves were collected from at least five plants from each treatment. The leaves were washed first with deionised water containing a non-ionic detergent, then with 0.01 M HCl and finally rinsed three times with deionised water. The material was dried at 60 °C until constant weight, weighed and then ground for analysis. The Fe concentration was determined by atomic absorption spectrophotometry (Pye Unicam, Cambridge, UK) after dry-ashing at 550 °C and digestion in HNO_3 and HCl following the AOAC (1990) procedure. Leaf Fe contents (μg) were calculated by multiplying the dry weight of each leaf by its corresponding Fe concentration.

2.3. Chlorophyll fluorescence measurements

Chl fluorescence imaging of leaves was performed using a blue version of the mini chlorophyll fluorometer–IMAG-MIN/B (Walz, Effeltrich, Germany). Pixel value images of the fluorescence parameters were displayed with the help of a false colour code ranging from black (0.000) through red, yellow, green, blue to pink (ending at 1.000). Chl *a* fluorescence parameters were assessed by the saturation pulse method in the most recently expanded leaf of five plants from each treatment. To evaluate spatial and temporal heterogeneity, four areas of interest (AOI, circle diameter 3 mm) were selected, one in the midrib of each leaf (AOI2) and three in interveinal areas (AOIs 1, 3 and 4). Leaves were dark-adapted for 15 min, and then images of basal fluorescence (F_0) were obtained by applying measuring light pulses modulated at 1 Hz, while images of the maximal fluorescence yield (F_m) were obtained with the help of a saturating blue pulse (6000 μmol m^{-2} s^{-1} PPFD) at 10 Hz. Based on F_0 and F_m, the images of maximum quantum efficiency of PSII photochemistry F_v/F_m, were derived as $(F_m - F_0)/F_m$. Afterwards, actinic illumination (205 μmol photons m^{-2} s^{-1}) was switched on and saturating pulses were applied at 20 s intervals for 5 min in order to determine the maximum fluorescence yield (F_m') and the chlorophyll fluorescence yield (F_s) during illumination. The photochemical efficiency of open PSII reaction centres or the intrinsic PSII efficiency was estimated by the ratio F_v'/F_m' and was calculated by measuring the same parameters as above on light-adapted leaves (F_0' and F_m'). The value of F_0' was estimated using the approximation of Oxborough and Baker (1997): $F_0' = F_0/(F_v/F_m + F_0/F_m')$. On light-adapted state, the quantum yield of PSII photochemistry, ϕ_{II}, was calculated by the $(F_m' - F_s)/F_m' = (\Delta F/F_m')$ ratio (Genty et al., 1989), whereas the photochemical quenching (q_p), which was used as an estimate of the fraction of open centres, was calculated as: $q_p = 1 - (F_s - F_0')/(F_m' - F_0')$ (Bilger and Schreiber, 1986). The electron transport rate (ETR) was estimated as: ETR = $\phi_{II} \times$ PPFD $\times$ 0.5 $\times$ absorptance, assuming an equal light distribution between PSII and PSI (Krall and Edwards (1992). The leaf absorptance values reported in Morales et al. (1991) were used as a proxy for Fe-deficient strawberry leaves. The utilization of absorbed photons by the PSII antennae in photosynthetic electron transport and thermal dissipation were assessed from the quantum yields of photochemical energy dissipation (ϕ_{II}), regulated (ϕ_{NPQ}) and non-regulated (ϕ_{NO}) thermal energy dissipation, with $\phi_{II} + \phi_{NPQ} + \phi_{NO} = 1$ assuming that the PSII pigments are organized according to the "Lake model" (Kramer et al., 2004). ϕ_{NPQ} and ϕ_{NO} in PSII were calculated by the equations $\phi_{NPQ} = 1 - \phi_{II} - 1/[NPQ + 1 + q_L(F_m/F_0 - 1)]$ and $\phi_{NO} = 1/[(NPQ + 1 + q_L)\ (F_m/F_0 - 1)]$, with $q_L = (F_m' - F_s)/(F_m' - F_0') \times F_0'/F_s = q_p \times F_0'/F_s$. The NPQ parameter was calculated according to the equation: $NPQ = (F_m - F_m')/F_m'$. As values of NPQ can be greater than one, images displayed correspond to NPQ/4, in order to be <1.000 and to allow the use of standard false colour code which values range from 0 to 1.

Rapid light curves (RLCs) were recorded after each measurement of the chlorophyll fluorescence kinetics, by exposing strawberry leaves to a sequence of actinic irradiances (0–700 μmol photons m^{-2} s^{-1}) in 12 discrete PPFD steps, each one lasting for 10 s. Images of F_s and F_m' were acquired at the end of each illumination step, from which automatically images of ETR, ϕ_{II}, ϕ_{NPQ} and ϕ_{NO} were calculated by the Imaging Win software. Light curves were constructed by averaging data from selected areas of interest in the corresponding images obtained from five plants of each treatment.

2.4. Data analysis

Statistical analysis and graphic display were performed with SPSS® (Release 16.0, SPSS Inc., Chicago, IL) and SigmaPlot® (Version 10.00, Systat Software, Inc. San Jose, CA, USA) software packages, respectively. All the determinations were obtained with randomly chosen plants. Since no significant differences were found between the values of the three interveinal selected areas of interest (AOIs), quantitative and statistic analyses were performed on the pooled data of the three AOIs. The Student's *t*-test was used for the comparison of the two groups. Comparisons among multiple groups were performed by one-way ANOVA after testing for normality and homogeneity of variance. Differences were considered significant if $P < 0.05$. When ANOVA yielded a significant *F* value, the individual means were compared using the Student–Newmans–Keul test (SNK).

3. Results

3.1. Degree of chlorosis and Fe contents

In Fe(+) plants no significant differences were recorded in Chl concentrations throughout the experimental period (data not shown). Typical symptoms of Fe deficiency appeared progressively in young leaves of the (Fe-) treatment, characterized by diffuse chlorosis in the interveinal regions. Based on Chl concentrations, leaves were allocated to four chlorosis degrees: Fe sufficient (621 – 551 μmol Chl cm^{-2}), moderately deficient (386.0 μmol Chl cm^{-2}), severely deficient (91.2 μmol Chl cm^{-2}) and extremely deficient (34.9 μmol Chl cm^{-2}) as shown in Fig. 1. In youngest fully expanded apical leaves, Chl concentration decreased progressively from 620.9 μmol m^{-2} to 34.9 μmol m^{-2}, and by day 42 the average value was only 6% of that of Fe(+) plants. In the Fe(−) treatment, plants also had less leaves with lower fresh and dry weights, and lower Fe content compared to Fe(+) plants (Table 1).

Iron resupply to the nutrient solution led to increases in Chl concentrations, which changed within eight days to values non-significantly different from those of Fe(+) plants (Fig. 1). Remarkably, recovered plants had the greatest Fe concentration, leading to a Fe content that was similar to that of Fe(+) plants (Table 1).

3.2. PSII photochemistry

Different parameters were measured in Fe-sufficient Fe(+), Fe-deficient Fe(−) and Fe-recovered Fe(−/+) strawberry plants to determine the effects on photosynthesis and the mechanisms of photoprotection. Colour-coded Chl fluorescence images of F_v/F_m, ϕ_{II}, NPQ/4 and q_p from representative individual leaves of Fe(+), Fe(−) and Fe(−/+) plants in each day are shown in Fig. 2. In Fe(+) leaves there were no significant differences during the experimental period and the image corresponding to time 0 was chosen to illustrate the pattern obtained. The images showed a noteworthy heterogeneous pattern of light utilization and photosynthetic activity, particularly at day 42 in Fe(−) plants, with higher values in midribs than in interveinal areas (Table 2). The images also revealed a homogeneous pattern of distribution of the maximum quantum

Table 1
Number, weight and Fe concentration and content of young leaves at the end of the experiment (day 50).

	Number of leaves	FW (g)	DW (g)	Fe concentration (mg kg^{-1} DW)	Fe content (μg leaf^{-1})
Fe(+)	4.4 a	7.67 a	1.45 a	65.3 b	94.4 a
Fe(−)	3.0 c	1.72 c	0.33 c	57.7 b	19.3 b
Fe(−/+)	3.6 b	6.02 b	1.02 b	120.3 a	122.7 a

Data are mean ± SE (n = 5). For each column, means with different letters indicate significant differences at P < 0.05 (SNK test). DW, dry weight; FW, fresh weight.

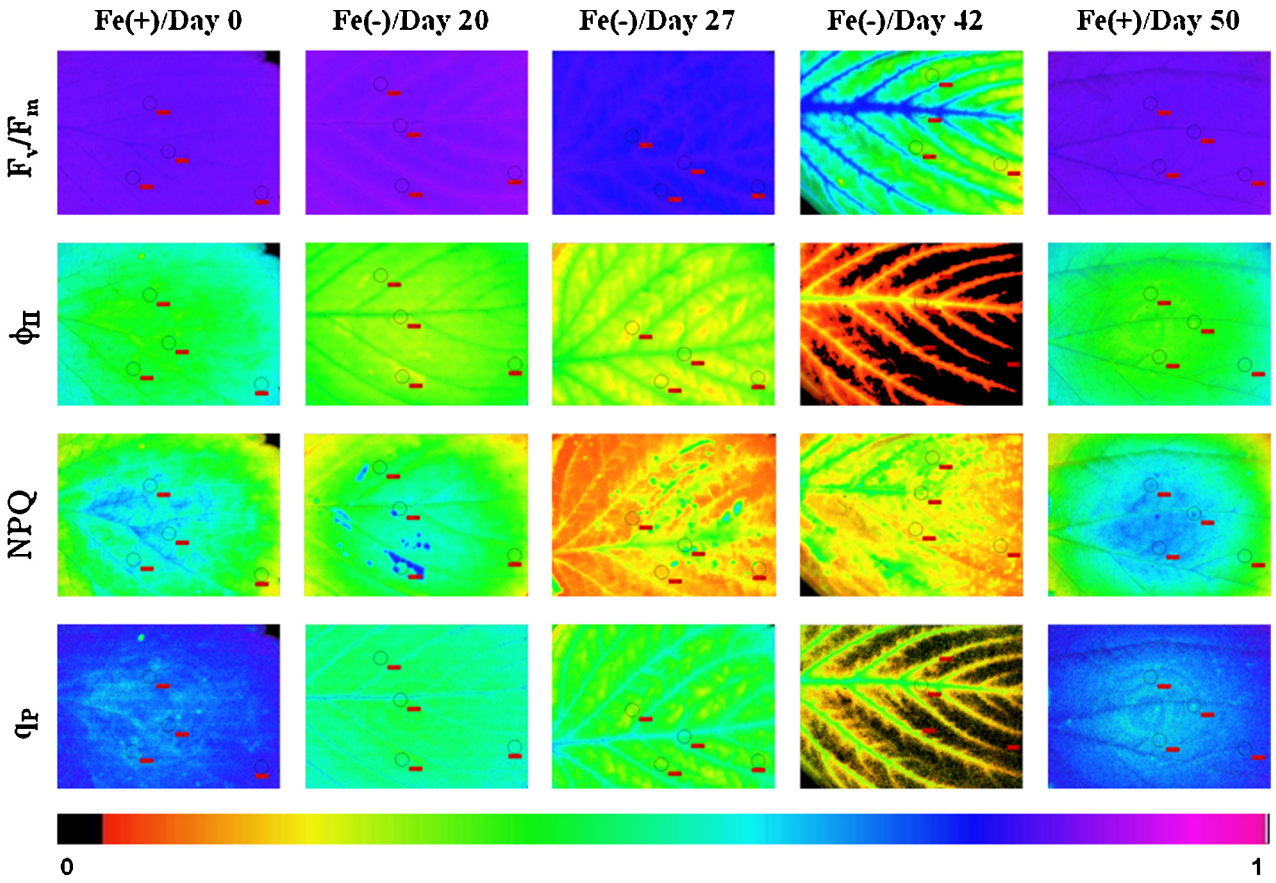

Fig. 2. Images of maximum quantum yield of PSII photochemistry (F_v/F_m), quantum yield of PSII electron transport in the light (ϕ_{II}), nonphotochemical quenching (NPQ/4) and photochemical quenching (q_p) at steady-state during Fe treatments (as in Fig. 1). Images are color coded according to the pattern (0 to 1) shown below the images. For each selected sample leaf, 4 areas of interest (AOIs) were defined and displayed as small circles in each image.

Table 2
Effects of Fe treatments (as in Fig. 1) on maximum and minimum fluorescence yield in dark (F_m and F_0, respectively), maximal photochemical efficiency of PSII (F_v/F_m), photochemical quenching (q_p), intrinsic PSII efficiency (F_v'/F_m'), quantum yield of PSII photochemistry (ϕ_{II}) and non photochemical quenching (NPQ) of midrib and interveinal leaf areas.

Chl fluorescence parameters	Leaf area	Fe(+)/Day0	Fe(−)/Day20	Fe(−)/Day27	Fe(−)/Day42	Fe(−/+)/Day50
F	Midrib	0.498 ± 0.012c*	0.781 ± 0.030a	0.681 ± 0.013b	0.747 ± 0.013a*	0.520 ± 0.014c
	Interveinal	0.525 ± 0.005b	0.715 ± 0.054a	0.703 ± 0.006a	0.697 ± 0.020a	0.526 ± 0.009b
F_0	Midrib	0.093 ± 0.001c	0.132 ± 0.024bc	0.167 ± 0.011b	0.271 ± 0.030a**	0.089 ± 0.006c
	Interveinal	0.097 ± 0.001c	0.127 ± 0.016c	0.187 ± 0.005b	0.433 ± 0.025a	0.090 ± 0.003c
F_v/F_m	Midrib	0.813 ± 0.005a	0.827 ± 0.036a	0.755 ± 0.014a	0.639 ± 0.034b***	0.829 ± 0.004a
	Interveinal	0.816 ± 0.003a	0.802 ± 0.036a	0.734 ± 0.008b	0.375 ± 0.035c	0.829 ± 0.004a
q_p	Midrib	0.705 ± 0.010a	0.470 ± 0.050c	0.457 ± 0.016c**	0.316 ± 0.035d**	0.571 ± 0.027b
	Interveinal	0.699 ± 0.006a	0.438 ± 0.051c	0.378 ± 0.012c	0.078 ± 0.031d	0.598 ± 0.018b
F_v'/F_m'	Midrib	0.592 ± 0.010a	0.648 ± 0.051a	0.596 ± 0.015a	0.473 ± 0.039b**	0.593 ± 0.016a
	Interveinal	0.595 ± 0.008a	0.646 ± 0.039a	0.596 ± 0.010a	0.282 ± 0.035b	0.609 ± 0.010a
ϕ_{II}	Midrib	0.417 ± 0.004a	0.350 ± 0.024b	0.272 ± 0.009c**	0.152 ± 0.026d***	0.338 ± 0.014b
	Interveinal	0.416 ± 0.008a	0.340 ± 0.025b	0.225 ± 0.007c	0.033 ± 0.014d	0.364 ± 0.012b
NPQ	Midrib	1.998 ± 0.091a	1.969 ± 0.233a	1.008 ± 0.078b*	0.974 ± 0.105b*	2.338 ± 0.151a
	Interveinal	2.032 ± 0.752a	1.267 ± 0.240b	0.814 ± 0.048c	0.664 ± 0.052c	2.126 ± 0.085a

Data are mean ± SE (n = 5). For each line, mean values followed by different letters are significantly different at P < 0.05 (SNK test).
* Indicates significant differences at P < 0.05 between midrib and interveinal areas (t-test) for each treatment and parameter.
** Indicates significant differences at P < 0.01 between midrib and interveinal areas (t-test) for each treatment and parameter.
*** Indicates significant differences at P < 0.001 between midrib and interveinal areas (t-test) for each treatment and parameter.

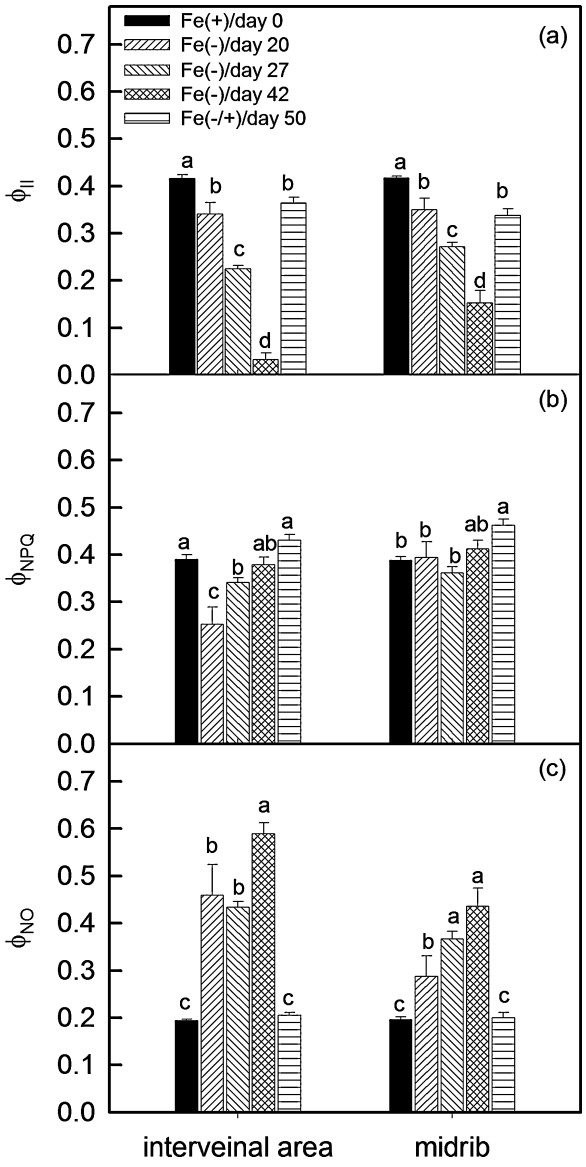

Fig. 3. Changes in (a) photochemical (ϕ_{II}), (b) regulated (ϕ_{NPQ}) and (c) non-regulated (ϕ_{NO}) energy dissipation in midrib and interveinal areas of leaves during Fe treatments (as in Fig. 1). Values shown are means ± SE of fifteen measurements taken in four areas of interest (AOIs) of five leaves per treatment. Different letters indicate significant differences between treatments ($P < 0.05$) according SNK test.

efficiency of PSII photochemistry over the screened leaf area, as estimated by the fluorescence ratio F_v/F_m of dark-adapted leaves, until day 42, when plants had lost over 90% of their chlorophyll (Fig. 1).

Leaves of Fe-sufficient Fe(+) and Fe-recovered Fe(−/+) plants had mean values of 0.822 ± 0.004 for maximum quantum efficiency of PSII photochemistry, irrespective of the area considered (Table 2). The value of F_v/F_m remained stable throughout the Fe deprivation period until day 42. However, a noticeable reduction in F_v/F_m was found in those extremely Fe-deficient leaves, mainly in consequence of significant increases in F_0 (Table 2). The effects were more drastic in the interveinal regions exhibiting visible symptoms of chlorosis (−54%) and less severe in the midrib (−22%). More evident differences between Fe(+) and Fe(−) plants were observed when the leaves were illuminated. Actual efficiency of PSII at steady state (ϕ_{II}), photochemical quenching (q_p) and non-photochemical quenching (NPQ) were affected early on, showing noticeable heterogeneities by day 27, with higher values in the midrib (Table 2), when chlorophyll concentration decreased by 38% (Fig. 1). Despite their spatial homogeneity by day 20, q_p and ϕ_{II} were significantly affected, with reductions of about 33% in q_p, while in ϕ_{II} the reduction reached only 15% (Table 2). By day 42, extremely Fe-deficient strawberry leaves had the lowest values of q_p, ϕ_{II} and NPQ, particularly in interveinal areas. The decrease of ϕ_{II} was caused not only by decreases in the proportion of open, i.e. oxidized PSII reaction centers, estimated by q_p, but also by decreases in intrinsic PSII efficiency (F_v'/F_m'). In the preceeding stages, the value of ϕ_{II} was affected exclusively by q_p, because F_v'/F_m') was constant ($\phi_{II} = q_p \times F_v'/F_m'$) (Table 2). At day 42, leaves were damaged and the symptomatic areas in the interveinal regions had values of ϕ_{II} and q_p close to zero (Fig. 2, Table 2).

Changes in chlorophyll fluorescence induced in Fe-deficient strawberry plants were fully reversible within a few days upon Fe resupply (Fig. 2, Table 2). Almost all fluorescence parameters returned to levels similar to those obtained in Fe(+) leaves on the 8th day following Fe resupply (day 50), but ϕ_{NPQ} was higher, which was reflected in a concurrent reduction of ϕ_{II}.

3.3. Photosynthetic energy partitioning

The contribution of the different pathways to energy partitioning in PSII complexes is shown in Fig. 3. Iron deficiency reduced the photochemical efficiency of PSII in light-adapted leaves (ϕ_{II}) in both leaf regions checked, with a more drastic effect in the interveinal areas than in the midrib. At day 42, the decrease in ϕ_{II} was about 64% in the midrib of Fe(−) leaves, while in the interveinal area the decrease reached 92%. This pronounced decrease in ϕ_{II} resulted from changes in the total non-photochemical quenching capacity ($\phi_{NPQ} + \phi_{NO}$). In midribs the pattern of quantum yield of regulated energy dissipation (ϕ_{NPQ}) was quite similar in all screened leaf areas, and ϕ_{NPQ} values remained relatively stable till recovery (day 50), when a significant increase occurred. In contrast, in interveinal areas, ϕ_{NPQ} values displayed variability throughout the study and showed some heterogeneity. In fact, ϕ_{NPQ} values decreased significantly in a first phase (day 20), and then began to increase until it reached values that were not significantly different from the Fe-sufficient treatment at days 42 and 50. Quantum yield of non-regulated energy dissipation (ϕ_{NO}) was enhanced considerably by Fe deprivation, with the highest values in extremely deficient plants. One week after Fe resupply, ϕ_{NO} returned to values analogous to those of Fe(+) plants, but ϕ_{II}, despite a significant increase in their values, did not recover completely because values of ϕ_{NPQ} remained high.

3.4. Rapid light curves (RLCs)

The response from ETR and other fluorescence parameters to photosynthetic photon flux density (PPFD) has been employed as a rapid and non-invasive probe to assess photosynthetic responses to light under Fe-stress conditions. Iron deficiency affected the light response curves of PSII activity (ETR, q_p and NPQ) as illustrated in Fig. 4. The observed patterns in the light-response curves (LCs) show that Fe deficiency decreased photosynthetic capacity, which reached the lowest value by day 42. As seen in Fig. 4A, the electron transport rate (ETR) increased similarly with PPFD in both Fe(+) leaves and in moderately Fe-stressed leaves (days 0, 20, respectively), and less intensely in severely Fe-stressed leaves (day 27). However, in extremely Fe-stressed leaves (day 42) the maximal ETR occurred at particularly low PPFD values. Photochemical quenching (q_p), as well as ETR, was consistently higher in Fe(+) leaves and moderately Fe-deficient leaves than in severely and extremely-deficient leaves (Fig. 4B). Plants developed non-photochemical quenching (NPQ) with increasing light intensity in all treatments (Fig. 4C). The NPQ increase was considerably higher in Fe(+) plants than in Fe(−)

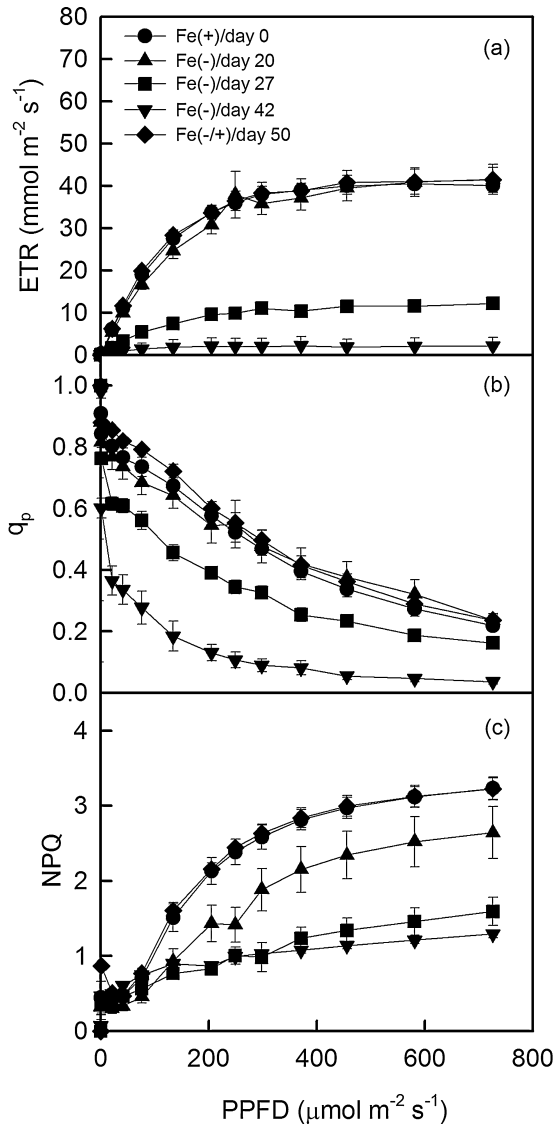

Fig. 4. The response of fluorescence parameters to PPFD during Fe treatments (as in Fig. 1). (a) Electron transport rate through PSII (ETR), (b) photochemical quenching (q_p), (c) non-photochemical quenching (NPQ). Data are means ± SE of five replicates per treatment.

plants. Moreover, in the latter, the increase in NPQ was much more pronounced in moderately Fe-stressed plants than in severely and extremely Fe-stressed plants. All measured fluorescence parameters reached their near-normal values after Fe stress alleviation (day 50), with the exceptions of ϕ_{II} and q_p, where recovery was only partial (Table 2).

4. Discussion

In this study, fluorescence imaging was used to provide early information on the effects induced by Fe omission or resupply on photosynthetic efficiency of strawberry plants. The images revealed spatial and temporal changes in photosynthetic efficiency of strawberry leaves under progressive Fe deficiency. They showed that the inhibition of photosynthesis was linked with Fe stress, and allowed the identification of localised areas that were more susceptible (interveinal mesophyll) or more resistant (midrib and veins) to Fe-stress.

Signs of chlorosis appeared first in interveinal areas, while midrib and veins remained green even in severely deficient leaves. Concurrently, the results obtained indicate that changes observed in the Fe content and concentrations were accompanied by parallel changes in total Chl concentration, suggesting a close relationship between the two variables. These findings are consistent with a study by Jiménez et al. (2009), who found that the Fe concentration was lower in mesophyll leaf areas than in midrib and veins in a *Prunus* hybrid under controlled conditions, which could be associated with chlorophyll concentration and chlorosis symptoms.

It has been shown that Fe deficiency causes both reductions in the number of photosynthetic units per area and decreases in intrinsic efficiency of remaining PSII units (Morales et al., 1998, 2000; Larbi et al., 2006). *Fragaria* × *ananassa* cv 'Diamond' appears to function normally under severe Fe stress (27 days) as indicated by values of F_v/F_m close to those typical of healthy leaves (0.83–0.76). In fact, Fe deficiency did not lead to sustained decreases in the maximal photochemistry efficiency (F_v/F_m) of strawberry leaves until they had lost most of their chlorophyll (92%), i.e. at extreme Fe deficiency (day 42). Even in this case, the decline of F_v/F_m was only 54% in interveinal areas and no more than 21% in the midrib. Data reported here show that the reductions on chlorophyll concentration during the period of Fe withholding were not associated with similar declines of the maximal photochemistry efficiency till day 42, suggesting photoinhibitory effects only when the Chl concentration was very low. Strong Fe deficiency could increase the susceptibility of PS II towards photoinhibition mainly through the decrease in leaf chlorophyll (Pätsikkä et al., 2002), which causes the amount of photons absorbed per chlorophyll unit to be markedly higher in Fe-deficient leaves (Morales et al., 2006). However, Fe-deficient leaves are to some extent protected against high PPFD by: (i) manifest decreases in light absorptance (40–80%), associated with decreases in chlorophyll and carotenoids; (ii) rises in light reflectance and transmittance, caused by changes in cuticle composition and in leaf optical properties (Morales et al., 2006 and references therein). Usually, signs of photoinhibitory damages were visible only in severely Fe-deficient plants with very low Chl concentration, which lead us to conclude that they may result from an imbalance between photoprotection and photoinhibiton mechanisms associated to leaf Chl and carotenoids concentrations. The fact that in extremely Fe-deficient strawberry plants, leaf interveinal areas with low chlorophyll were photoinhibited faster and more markedly than high chlorophyll leaf midribs adds support to this interpretation. Data also showed that changes in F_v/F_m under extreme Fe stress were caused by an increase of minimal chlorophyll fluorescence (F_0), which is usually an indicator of disconnection of the light-harvesting antennae from their reaction centers (Moseley et al., 2002; Larbi et al., 2006). However, in Fe-deficient leaves F_v/F_m ratios can be underestimated due to the presence of some closed PS II reaction centers in dark adapted Fe-deficient leaves (Belkhodja et al., 1998). Consequently, a constant PSII fluorescence emission in dark-adapted leaves of Fe-deficient leaves (~15%) can lead to an underestimation of the F_v/F_m ratios (Morales et al., 2001). Thus, the protocol for measuring Chl fluorescence must incorporate a brief period of far-red illumination before darkness, to remove electrons from the acceptor site which causes the modulated fluorescence yield to decline to true F_0 levels. Unfortunately, the Chl fluorescence imaging device does not apply far-red, and F_v/F_m in Fe-deficient leaves were probably underestimated. Nevertheless, in extremely Fe-deficient strawberry plants the F_v/F_m drop was so drastic that after removing the constant fluorescence emission the values were still significantly lower than those obtained in Fe-sufficient plants. Although several reports suggested that moderate Fe deficiency could decrease F_v/F_m (Morales et al., 1991; Pestana et al., 2005, 2011b), other studies (Morales et al., 2000, 2001) showed that persistent decreases in PSII efficiency occurred only with severe Fe deficiency, which is in agreement with our results. This apparent discrepancy could be

due to inaccurately high F_0 values, related to the reduction of the plastoquinone (PQ) pool in the dark, which magnitude depends on the level of Fe chlorosis and on the duration of pre illumination and dark-adaptation (Belkhodja et al., 1998; Morales et al., 2006). Chlorophyll fluorescence images of strawberry leaves also revealed that F_v/F_m decreased differentially in various parts of the leaf. Under extreme Fe stress, F_v/F_m decreased less in the midrib than in interveinal areas, which led us to conclude that the signs of photoinhibitory damage were particularly drastic in interveinal areas.

The deleterious effects of Fe deficiency on photosynthetic efficiency emerged earlier under growth light intensities than in the dark. Quantum yield at light (ϕ_{II}) decreased significantly by day 20 in both midrib and interveinal tissues. This indicates that the mechanisms of energy dissipation were engaged and electron transport was depressed early on during the Fe deprivation period. Further support for that comes from the light response curves of ETR. As previously reported for sugar beet (Morales et al., 1991), in strawberry leaves the response of ϕ_{II} to Fe deficiency was also biphasic. In a first phase, when leaves lose a large part of their chlorophyll, the decline in the fraction of open centers, reflected in a decrease of q_p, was the only factor leading to the depression of ϕ_{II}. Nevertheless, the closed centers may work quite efficiently if opened, as shown by the relatively high F_v'/F_m' values. In a second phase, when the Fe stress was extreme, chlorophyll decreased by up to 90% (day 42) and a disconnection of the light-harvesting antennae from their action centers was detected (increase of F_0); a smaller excitation capture efficiency of PSII (F_v'/F_m') also contributed to the decrease of ϕ_{II}. However, while in sugar beet and other species (Abadía et al., 1999), PS II reaction centers were protected against excess light by enhanced energy dissipation in PSII associated to de-epoxidation of violaxanthin (increases in NPQ), in strawberry it seems that this process may not be the main way to dissipate excess excitation energy in Fe-deficient leaves. Changes in energy dissipation can be followed by increases in NPQ and/or in $1 - F_v'/F_m$ (Demmig-Adams et al., 1996), but NPQ may also reflect a disconnection of part of the antenna, which also photoprotects the PSII reaction centers (Peguero-Pina et al., 2013). In this study, although no increase in NPQ was evident, a decrease in F_v'/F_m' was detected, hence it should be concluded that the energy dissipation was enhanced under Fe deficiency. One can speculate that because of the structural disconnection of part of the PSII antenna in severely Fe-deficient leaves (Morales et al., 2001), the NPQ (reflecting functional and reversible disconnection, in addition to thermal dissipation) would be less able to show thermal dissipation than F_v'/F_m'. The effects were more visible in the interveinal areas than in midrib, which indicates that there was a greater potential for restriction in photosynthesis and suppression of the protective ability of total non-photochemical mechanisms in the interveinal areas than in the veins. Moreover, quantitative analysis of the energy partitioning in PSII complexes, performed according to the model of Kramer et al. (2004), proved that Fe deficiency modified the fate of absorbed light energy within PSII. Our findings showed that when Fe deficiency increased, the decline of ϕ_{II} was accompanied by a clear increase in ϕ_{NO} (50–60% of the total flux in interveinal areas), without appreciable changes in ϕ_{NPQ} (midrib) or decreases in moderate Fe deficiency (interveinal areas). Therefore, the availability of alternative electron sink(s) and/or additional quenching mechanism(s) might play an important role in the dissipation of excess light energy when the capacity for the upregulation of the primary zeaxanthin-regulated nonphotochemical quenching (ϕ_{NPQ}) pathway is restricted at low Fe level. However, those alternative routes can cause an overproduction of reactive oxygen species (ROS) and Chl* with potential for photodamage of PSII. Although the higher ϕ_{NO} in Fe-deficient plants points to a higher proportion of inactive and/or damaged PSII centres compared with the Fe-sufficient plants, it may also have a positive effect by providing effective energy dissipation and photoprotection to the remaining functional PSII units. Anyway, it is indicative of the plant having serious problems in coping with the incident radiation, because either it is already damaged or will be photodamaged upon further irradiation. Therefore, if no Fe were provided to extremely Fe-deficient strawberry plants, the photosynthetic apparatus would be irreversibly affected and yield and fruit quality losses could be considerable.

In our study, Fe-deficient strawberry plants resupplied with Fe showed a reversal of all the parameters within eight days, resulting in total leaf re-greening and increases in chlorophyll *a* fluorescence. Similar effects have been reported in annual species, for instance in sugar beet (Larbi et al., 2004), chickpea (Mahmoudi et al., 2007) and tomato (Tomasi et al., 2009). The short resupply period led also to an efficient Fe accumulation in young leaves, which showed Fe content similar to that of plants grown with a sufficient supply of Fe during the whole experiment. It was reported that Fe resupply to annual Fe-deficient species leads within a few days to increases in chlorophyll (Chl) concentrations and photosynthetic activity (Nishio et al., 1985; Larbi et al., 2004). It can be speculated that when plants are resupplied with Fe some of the mechanisms elicited by Fe-deficiency will be modulated or de-activated in the short term. The increase in Chl concentration, which indicates de novo Chl biosynthesis, and probably of protein composition, leads to a rapid re-organization of the chloroplast structure, and function of the entire photosynthetic apparatus. However, in extremely Fe-deficient strawberry plants, even eight days after Fe was restored, a considerable fraction of energy was still dissipated thermally (high ϕ_{NPQ}), which is consistent with the observed incomplete recovery of ϕ_{II}. These results may be interpreted as an enhanced capacity for photoprotection by downregulation of the photosynthetic efficiency while the complete restoration of the photochemical apparatus takes place.

5. Conclusions

In summary, Chl fluorescence imaging proved to be a useful technique to investigate the plant photosynthetic performance under progressive Fe stress and recovery after Fe resupply. Furthermore, it was shown that the effects of different degrees of Fe stress on strawberry leaves generate spatio-temporal heterogeneity in fluorescence response, pointing out the inadequacy of using single time or single point leaf analyses to monitor Fe deficiency. The results from this study also suggest that ϕ_{II} measured in the interveinal tissue could be a better indicator for an early and fast detection of Fe deficiency than F_v/F_m, and could be applied for fertilization management.

Acknowledgments

This study was funded by the National Project from the FCT (PTDC/AGR-PRO/3861/2012). M.L. Osório acknowledges a grant from the Portuguese Science and Technology (FCT, SFRH/BPD/35410/2007). We wish to thank Florinda Gama and Teresa Saavedra for excellent technical assistance.

References

Abadía, J., Morales, F., Abadía, A., 1999. Photosystem II efficiency in low chlorophyll, iron-deficient leaves. Plant Soil 215, 183–192.

Abadía, J., Vázquez, S., Rellán-Álvarez, R., El-Jendoubi, H., Abadía, A., Álvarez-Fernández, A., López-Millán, A.F., 2011. Towards a knowledge-based correction of iron chlorosis. Plant Physiol. Biochim. 49, 471–482.

AOAC, 1990. In: Hedrich, K. (Ed.), Official Methods of Analysis of the Association of Official Analytical Chemists. Academic, Washington, DC, p. 1141.

Baker, N.R., 2008. Chlorophyll fluorescence: a probe of photosynthesis in vivo. Annu. Rev. Plant Biol. 59, 89–113.

Belkhodja, R., Morales, F., Quílez, R., López-Millán, A.F., Abadia, A., Abadia, J., 1998. Iron deficiency causes changes in chlorophyll fluorescence due to the reduction in the dark of the Photosystem II acceptor side. Photosynth. Res. 56, 265–276.
Bilger, W., Schreiber, U., 1986. Energy-dependent quenching of dark-level chlorophyll fluorescence in intact leaves. Photosynth. Res. 10, 303–308.
Calatayud, A., Roca, D., Martínez, P.F., 2006. Spatial-temporal variations in rose leaves under water stress conditions studied by chlorophyll fluorescence imaging. Plant Physiol. Biochem. 44, 564–573.
Demmig-Adams, B., Adams III, W., Barker, D.H., Logan, B.A., Bowling, D.R., Verhoeven, A.S., 1996. Using chlorophyll fluorescence to assess the fraction of absorbed light allocated to thermal dissipation of excess excitation. Physiol. Plant 98, 253–264.
Genty, B., Briantais, J.M., Baker, N.R., 1989. The relationship between the quantum yield of photosynthetic electron transport and quenching of chlorophyll fluorescence. Biochim. Biophys. Acta 990, 87–92.
Gorbe, E., Calatayud, A., 2012. Applications of chlorophyll fluorescence imaging technique in horticultural research: a review. Sci. Hortic. 138, 24–35.
Hecht-Buchholz, C.H., Ortmann, U., 1986. Effect of foliar iron application on regreening and chloroplast development in iron chlorotic soybean. J. Plant Nutr. 9, 647–659.
Jiménez, S., Morales, F., Abadía, A., Abadía, J., Moreno, M.A., Gogorcena, Y., 2009. Elemental 2-D mapping and changes in leaf iron and chlorophyll in response to iron re-supply in iron-deficient GF 677 peach–almond hybrid. Plant Soil 315, 93–106.
Klughammer, C., Schreiber, U., 2008. Complementary PS II quantum yields calculated from simple fluorescence parameters measured by PAM fluorometry and the Saturation Pulse method. PAM Appl. Notes 1, 27–35.
Kornyeyev, D., Hendrickson, L., 2007. Energy partitioning in photosystem II complexes subjected to photoinhibitory treatment. Funct. Plant Biol. 34, 214–220.
Krall, J.P., Edwards, G.E., 1992. Relationship between photosystem II activity and CO_2 fixation in leaves. Plant Physiol. 86, 180–187.
Kramer, D.M., Johnson, G., Kiirats, O., Edwards, G.E., 2004. New fluorescence parameters for the determination of QA redox state and excitation energy fluxes. Photosynth. Res. 79, 209–218.
Larbi, A., Abadía, A., Abadía, J., Morales, F., 2006. Down co-regulation of light absorption, photochemistry, and carboxylation in Fe-deficient plants growing in different environments. Photosynth. Res. 89, 113–126.
Larbi, A., Abadía, A., Morales, F., Abadía, J., 2004. Fe resupply to Fe deficient sugar beet plants leads to rapid changes in the violaxanthin cycle and other photosynthetic characteristics without de novo chlorophyll synthesis. Photosynth. Res. 79, 59–69.
Lichthentaler, H.K., Miehé, J.A., 1997. Fluorescence imaging as a diagnostic tool for plant stress. Trends Plant Sci. 2, 316–320.
Mahmoudi, H., Labidi, N., Ksouri, R., Gharsalli, M., Abdelly, C., 2007. Differential tolerance to iron deficiency of chickpea varieties and Fe resupply effects. C.R. Biol. 330, 237–246.
Martins, N., Osório, M.L., Gonçalves, S., Osório, J., Palma, T., Romano, A., 2013. Physiological responses of *Plantago algarbiensis* and *P. almogravensis* shoots and plantlets to low pH and aluminium stress. Acta Physiol. Plant 35, 615–625.
Morales, F., Abadía, A., Abadía, J., 1991. Chlorophyll fluorescence and photon yield of oxygen evolution in iron-deficient sugar beet (*Beta vulgaris* L.) leaves. Plant Physiol. 97, 886–893.
Morales, F., Grasa, R., Abadía, A., Abadía, J., 1998. Iron chlorosis paradox in fruit trees. J. Plant Nutr. 21, 815–825.
Morales, F., Belkhodja, R., Abadía, A., Abadía, J., 2000. Photosystem II efficiency and mechanisms of energy dissipation in iron-deficient, field-grown pear trees (*Pyrus communis* L.). Photosynth. Res. 63, 9–21.
Morales, F., Moise, N., Quílez, R., Abadía, A., Abadía, J., Moya, I., 2001. Iron deficiency interrupts energy transfer from a disconnected part of the antenna to the rest of Photosystem II. Photosynth. Res. 70, 207–220.
Morales, F., Abadía, A., Abadía, J., 2006. Photoinhibition and photoprotection under nutrient deficiencies, drought and salinity. In: Demmig-Adams, B., et al. (Eds.), Photoprotection, Photoinhibition, Gene Regulation, and Environment. Springer, The Netherlands, pp. 65–85.
Moseley, J.F., Allinger, T., Herzog, S., Hoerth, P., Wehinger, E., Merchant, S., Hippler, M., 2002. Adaptation to Fe-deficiency requires remodelling of the photosynthetic apparatus. EMBO J. 21, 6709–6720.
Nishio, J.N., Abadía, J., Terry, N., 1985. Chlorophyll-proteins and electron transport during iron nutrition-mediated chloroplast development. Plant Physiol. 78, 269–299.
Osório, M.L., Osório, J., Vieira, A.C., Gonçalves, S., Romano, A., 2011. Influence of enhanced temperature on photosynthesis, photooxidative damage, and antioxidant strategies in *Ceratonia siliqua* L. seedlings subjected to water deficit and rewatering. Photosynthetica 49, 3–12.
Osório, M.L., Osório, J., Gonçalves, S., David, M.M., Correia, J., Romano, A., 2012. Carob trees (*Ceratonia siliqua* L.) regenerated in vitro can acclimatize successfully to match the field performance of seed-derived plants. Trees 26, 1837–1846.
Osório, M.L., Osório, J., Romano, A., 2013. Photosynthesis, energy partitioning, and metabolic adjustments of the endangered Cistaceae species *Tuberaris major* under high temperature and drought. Photosynthetica 51, 75–84.
Oxborough, K., Baker, N.R., 1997. Resolving chlorophyll *a* fluorescence images of photosynthetic efficiency into photochemical and non-photochemical components—calculation of qP and $F_{v'}/F_{m'}$ without measuring F_0. Photosynth. Res. 54, 135–142.
Pätsikkä, E., Kairavuo, M., Šeršen, F., Aro, E.-M., Tyystjärvi, E., 2002. Excess copper predisposes photosystem II to photoinhibition in vivo by outcompeting iron and causing decrease in leaf chlorophyll. Plant Physiol. 129, 1359–1367.
Pestana, M., de Varennes, A., Abadía, J., Faria, E.A., 2005. Differential tolerance to iron deficiency of citrus rootstocks grown in nutrient solution. Sci. Hortic. 104, 25–36.
Pestana, M., de Varennes, A., Faria, E.A., 2004. Lime-induced iron chlorosis in fruit trees. In: Dris, R., Jain, S.M. (Eds.), Production Practices and Quality Assessment of Food Crops. Plant Mineral Nutrition and Pesticide Management, 2. Kluwer Academic Publishers, Dordrecht, The Netherlands, ISBN 1-4020-1699-9, p. 171.
Pestana, M., Domingos, I., Gama, F., Dandlen, S., Miguel, M.G., Pinto, J.C., de Varennes, A., Correia, P.J., 2011a. Strawberry recovers from iron chlorosis after foliar application of a grass-clipping extract. J. Plant Nutr. Soil Sci. 174, 473–479.
Pestana, M., Correia, P.J., David, M., Abadía, A., Abadía, J., de Varennes, A., 2011b. Response of five citrus rootstocks to iron deficiency. J. Plant Nutr. Soil Sci. 174, 837–846.
Pestana, M., Correia, P.J., Saavedra, T., Gama, F., Abadía, A., de Varennes, A., 2012. Development and recovery of iron deficiency by iron resupply to roots or leaves of strawberry plants. Plant Physiol. Biochim. 53, 1–5.
Peguero-Pina, J.J., Gil-Pelegrín, E., Morales, F., 2013. Three pools of zeaxanthin in *Quercus coccifera* leaves during light transitions with different roles in rapidly reversible photoprotective energy dissipation and photoprotection. J. Exp. Bot. 64, 1649–1661.
Pushnik, J.C., Miller, G.W., 1989. Iron regulation of chloroplasts photosynthetic function: mediation of PS I development. J. Plant Nutr. 12, 407–421.
Tomasi, N., Rizzardo, C., Monte, R., Gottardi, S., Jelali, N., Terzano, R., Vekemans, B., De Nobili, M., Varanini, Z., Pinton, R., Cesco, S., 2009. Micro-analytical, physiological and molecular aspects of Fe acquisition in leaves of Fe-deficient tomato plants resupplied with natural Fe-complexes in nutrient solution. Plant Soil 325, 25–38.
Terry, N., Abadía, J., 1986. Function of iron in chloroplasts. J. Plant Nutr. 9, 609–646.